

Antiwear Performance and Mechanism of an Oil-Miscible Ionic Liquid as a Lubricant Additive

Jun Qu,^{*,†} Dinesh G. Bansal,[†] Bo Yu,[‡] Jane Y. Howe,[†] Huimin Luo,[‡] Sheng Dai,[§] Huaqing Li,^{†,⊥} Peter J. Blau,[†] Bruce G. Bunting,[‡] Gregory Mordukhovich,[#] and Donald J. Smolenski[#]

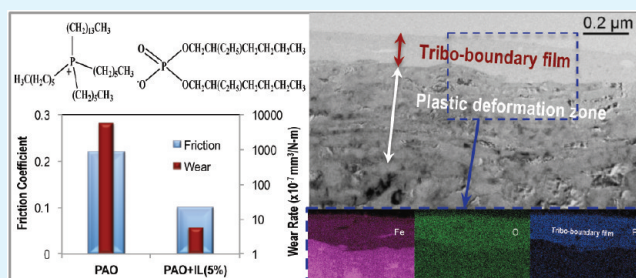
[†]Materials Science and Technology Division, [‡]Energy and Transportation Science Division, and [§]Chemical Sciences Division, Oak Ridge National Laboratory

[⊥]Department of Physics, University of Tennessee

[#]Research & Development Center, General Motors Corp.

ABSTRACT: An ionic liquid (IL) trihexyltetradecylphosphonium bis(2-ethylhexyl) phosphate has been investigated as a potential antiwear lubricant additive. Unlike most other ILs that have very low solubility in nonpolar fluids, this IL is fully miscible with various hydrocarbon oils. In addition, it is thermally stable up to 347 °C, showed no corrosive attack to cast iron in an ambient environment, and has excellent wettability on solid surfaces (e.g., contact angle on cast iron <8°). Most importantly, this phosphonium-based IL has demonstrated effective antiscaffing and antiwear characteristics when blended with lubricating oils. For example, a 5 wt % addition into a synthetic base oil eliminated the scuffing failure experienced in neat oil and, as a result, reduced the friction coefficient by 60% and the wear rate by 3 orders of magnitude. A synergistic effect on wear protection was observed with the current antiwear additive when added into a fully formulated engine oil. Nanostructure examination and composition analysis revealed a tribo-boundary film and subsurface plastic deformation zone for the metallic surface lubricated by the IL-containing lubricants. This protective boundary film is believed to be responsible for the IL's antiscaffing and antiwear functionality.

KEYWORDS: phosphonium-based ionic liquids, lubricants, additives, antiwear, boundary film, oil-solubility



1. INTRODUCTION

Lubrication regimes in mechanical devices such as engines can be divided into three general categories: boundary, mixed, and elastohydrodynamic/hydrodynamic lubrication, among which hydrodynamic lubrication has the lowest friction and wear. Modern engines are designed to minimize the contribution of boundary and mixed friction (although these losses cannot be totally eliminated) and their parasitic friction loss (accounting for 10–15% of the total engine-generated energy¹) is primarily induced by elastohydrodynamic drag between the piston rings and cylinder liners, which is proportional to the lubricant viscosity.

Developing more effective additive packages in combination with balancing lubricant viscosity has proven to be the most successful and cost-effective route to improving engine efficiency and durability. Commercial lubricants are composed of base stock and several categories of additives including antiwear, friction modifier, viscosity modifier, antioxidant, detergent, dispersant, etc.² Specifically, friction modifiers and antiwear agents play key roles in reducing boundary and mixed friction and wear in engine locations such as the top-ring-reversal region of the piston ring-cylinder liner interface and sliding surfaces in the valve train. Furthermore, an effective antiwear additive allows using a low viscosity lubricant, consequently reducing elastohydrodynamic friction loss.

Ionic liquids³ have been explored for lubrication applications since 2001.⁴ The majority of the literature has focused on using ILs as neat lubricants or base stocks, which would be suitable for special bearing applications such as for operation at >250 °C where conventional hydrocarbon lubricants start decomposing, but many ILs are stable. Another approach is to use ILs as lubricant additives, which has significant practical merit because it may get into the lubricant market without requiring major supply and distribution changes. However, most ILs have little or no solubility (<<1%) in nonpolar hydrocarbon oils. Most previous studies used unstable oil-IL emulsions or low concentrations of ILs in nonpolar base oils,^{5–12} and others used a polar base stock for better compatibility with ILs.^{13,14} Therefore, there is a significant opportunity for developing ILs with good solubility in nonpolar lubricating base oils.

In this paper, we report the results of research on the IL trihexyltetradecylphosphonium bis(2-ethylhexyl) phosphate, which is not only soluble but fully miscible in common nonpolar hydrocarbon oils. Results with this IL reported here have demonstrated high thermal stability, noncorrosiveness,

Received: November 23, 2011

Accepted: January 16, 2012

Published: January 16, 2012

and high effectiveness in reducing friction and wear when blended into lubricating oils. Surface boundary film examination revealed the antiwear mechanism for the IL additive and its synergistic effects with an existing additive package.

2. EXPERIMENTAL SECTION

Trihexyltetradecylphosphonium bis(2-ethylhexyl) phosphate ($[P_{66614}][DEHP]$), whose molecular structure is shown in Figure 1,

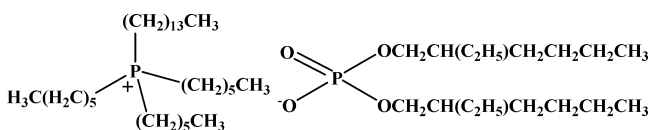


Figure 1. Trihexyltetradecylphosphonium bis(2-ethylhexyl) phosphate.

was synthesized following the procedure described by Sun et al.¹⁵ The feed stocks, including tetradecyl trihexyl phosphonium bromide, bis(2-ethylhexyl) hydrogen phosphate, and sodium hydroxide, were from Sigma-Aldrich Company LLC. In synthesis, 5.13 g (15.9 mmol) of bis(2-ethylhexyl) phosphate (HDEHP) was mixed with 8.96 g (15.9 mmol) of tetradecyl trihexyl phosphonium bromide in hexane. An aqueous solution of NaOH with equal molar to HDEHP was then added dropwise into the reaction system and the mixture was stirred at room temperature for 4 h. The organic phase was separated and washed with deionized water (18.2 MΩ cm) three times to ensure the removal of NaBr. The solvent was removed by rotary evaporation and the product was dried under vacuum at 70 °C overnight. The yield was ~95%.

Two hydrocarbon lubricating oils were used as base stock as well as baseline lubricants: (1) Mobil 1TM synthetic poly alpha-olefin (PAO) 4 cSt and (2) fully formulated Mobil 1TM SAE 5W-30 engine oil, which were kindly provided by Exxon Mobil Corp. Two oil-IL blends were prepared by adding 5 wt.% $[P_{66614}][DEHP]$ into the PAO base oil and the SAE 5W-30 engine oil, respectively.

Thermogravimetric analysis (TGA) was carried out on a TA Instruments TGA-2950 at a 10 °C/min heating rate in a nitrogen atmosphere. Kinematic viscosities of $[P_{66614}][DEHP]$ and oil-IL blends were measured in the temperature range of 0–100 °C using a Petrolab MINIVIS II viscometer.

The corrosivity of $[P_{66614}][DEHP]$ was investigated in both exposure tests and electrochemical evaluation. In the exposure test, a droplet of this IL was placed on a cast iron liner sample surface under ambient conditions for 2 months. The electrochemical measurement was conducted on a Gamry Instruments reference 600 potentiostat/galvanostat/ZRA to generate a potentiodynamic polarization curve. The cast iron working electrode had an exposed surface area of 0.61 cm² against a Pt counter electrode. Because of the small volume of fluid (~10 mL), Pt was used as a quasi-reference. The potential from –0.5 to 0.5 was scanned with a rate of 1 mV/s.

An optical tensiometer (KVS Instruments Theta T200) was used to measure the contact angles of the IL and oils on gray cast iron and AISI 52100 steel surfaces to compare their wetting performance, which is an important criterion for lubricant evaluation. Because the contact angle is sensitive to surface condition, such as flatness, roughness, and

cleanliness, all surfaces were prepared using the same metallographic polishing procedure to control the roughness in a narrow range of $R_a = 20–30$ nm.

The tribological performance of the IL additive in oil was evaluated using a reciprocating sliding test on a Plint TE77 (Phoenix Tribology Ltd.) high-frequency tribometer. The upper and lower specimens were cut from an engine piston steel ring and cast iron cylinder liner, respectively, provided by General Motors Corp. Tests were conducted at room temperature (~23 °C) under a normal load of 160 N and an oscillation frequency of 10 Hz with a 10 mm stroke for a sliding distance of 1000 m. This set of testing conditions were chosen to simulate the contact pressure and sliding speed at the top-ring-reversal region of the piston ring-cylinder liner interface. On the basis of the lubricant film thickness calculation,¹⁶ all tests were under boundary lubrication. At least two replicates were run for each lubricant. The friction coefficient was monitored in situ by capturing the tangential force (using a piezoelectric load cell) that was then divided by the normal load, and the wear rate, expressed in units of mm³/N-m, was quantified by measuring the wear volume (using a 3D optical interferometer Wyko NT9100) and normalized by the load and sliding distance.

The worn surface morphology was examined using a Hitachi S-4800 field-emission scanning electron microscope (SEM). Transmission electron microscopy (TEM), electron diffraction, and energy-dispersive X-ray spectroscopy (EDS) were used in cross-section examination to study the nanostructure and composition of the surface boundary film as well as the plastic deformation zone below it. The TEM samples were prepared using a FEI Nova 200 Dual-beam Focused Ion Beam (FIB) System with a Ga source to extract a thin cross-section of the near-surface zone from the wear scar of each specimen. The TEM system was a Hitachi HF-3300 TEM/STEM at 300 kV (1.3 Å resolution) equipped with a Bruker solid-state EDS detector with a 30 mm² window.

3. RESULTS AND DISCUSSION

3.1. Density, Viscosity, And Thermal Stability. The densities at room temperature, viscosities from zero to 100 °C, and TGA-determined decomposition temperatures for $[P_{66614}][DEHP]$, PAO and SW-30 oils, and their blends are summarized in Table 1. The IL has a slightly higher density (0.91 g/cm³) but is much more viscous compared with the oils. $[P_{66614}][DEHP]$ is hydrophobic and stable in presence of water. No noticeable degradation, e.g., discoloration, was observed when exposed to air at room temperature based on a 2-month exposure test. When heated, $[P_{66614}][DEHP]$ is more stable than hydrocarbon oils. TGA tests in a N₂ environment revealed an onset decomposition temperature of 347 °C for $[P_{66614}][DEHP]$ versus 250 and 263 °C for the PAO and SAE 5W-30 engine oils, respectively.

3.2. Corrosivity and Wettability. Unlike many other ILs for which corrosion is a concern due to their ionic nature, $[P_{66614}][DEHP]$ showed no corrosive attack to nonprotected metals. An active-passive behavior was observed in the electrochemical corrosion test. The potentiodynamic polarization curve in Figure 2 shows an active dissolution behavior from

Table 1. Comparison of Decomposition Temperature, Density, And Kinematic Viscosity^a

lubricant	decomp. temp. (°C)	density (g/mL 23 °C)	kinematic viscosity (cSt)				
			0 °C	10 °C	23 °C	40 °C	100 °C
PAO 4 cSt base oil	250	0.80	119.0	67.8	34.5	17.6	3.7
SW-30 engine oil	263	0.80	593.0	299.8	140.9	63.3	10.5
$[P_{66614}][DEHP]$	347	0.91	NA	NA	1045.1	429.0	49.5
PAO+IL(5 wt.%)	NM	0.81	122.8	69.9	36.6	18.4	3.8
PAO+IL(50 wt.%)	NM	0.86	752.8	391.9	187.1	88.3	13.0
SW-30+IL(5 wt.%)	NM	0.81	653.7	325.3	149.9	65.8	10.5

^aNA, viscosity above the upper limit (>1500 cP) of the measurable range of the instrument; NM, not measured.

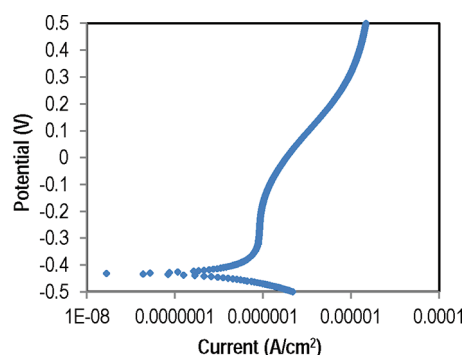


Figure 2. Potentiodynamic polarization curve of cast iron in $[P_{66614}][DEHP]$.

E_{corr} at -0.43 to -0.38 V followed by a region of weak passivation and a transpassive region, beyond which a second passive-transpassive cycle appears. In a simple exposure test, no pitting was observed on a cast iron surface that had a droplet of $[P_{66614}][DEHP]$ on it for 2 months (the end of test). $[P_{66614}][DEHP]$ is not only noncorrosive itself, but also help prevent rusting by its strong hydrophobicity.

$[P_{66614}][DEHP]$ showed excellent wetting behavior on gray cast iron and AISI 52100 bearing steel surfaces with contact angles of 7.6 and 20.7° , respectively. Its wettability on cast iron is significantly better than common imidazolium- and ammonium-based ILs⁶ and slightly outperforms the lubricating oils, as seen in Table 2.

Table 2. Comparison of Contact Angles

lubricant	gray cast iron	AISI 52100 steel
PAO 4 cSt base oil	13.0	22.4
5W-30 engine oil	9.0	23.9
$[P_{66614}][DEHP]$	7.6	20.7
$[C_{10}mim][Tf_2N]$ (ref. ⁶)	33.9	29.0
$[C_8H_{17}]_3NH][Tf_2N]$ (ref. ⁶)	22.2	16.2

3.3. Oil Miscibility. $[P_{66614}][DEHP]$ was found to be fully miscible with a variety of hydrocarbon lubricating oils, both petroleum-derived, such as SAE 10W base oil and SAE 10W30 engine oil, and synthetic, such as Mobil 1™ PAO base oil and SAE 5W-30 engine oil, and Royal Purple SAE 0W-10 racing engine oil. All oil-IL blends appear clear without clouds or phase separation by visual inspection over a large temperature range (from -18 to 175 °C). Most oils had no apparent color change after being blended with $[P_{66614}][DEHP]$, except for Mobil 1 5W-30 oil which changed from light brown to red (oil remaining clear) implying some reaction between $[P_{66614}][DEHP]$ and existing oil additives. Figure 3 compares the measured viscosities for PAO-IL blends in 95:5 and 50:50 ratios with the computed values using the Refutas equation¹⁷ that was derived for single-phase multiple-component liquids. The relatively good agreement confirms the oil-miscibility of $[P_{66614}][DEHP]$.

In general, ions and nonpolar neutral organic molecules are immiscible, because ions are attracted by polar forces, whereas nonpolar molecules are held together by dispersion forces. The exceptional oil-miscibility of $[P_{66614}][DEHP]$ is hypothesized to attribute to its three-dimensional quaternary structures with high steric hindrance (long hydrocarbon chains) that dilute the charge of the ions and therefore improve the compatibility with neutral oil molecules. In contrast, most ILs studied in the literature contain either two-dimensional cations, e.g., imidazolium-based,

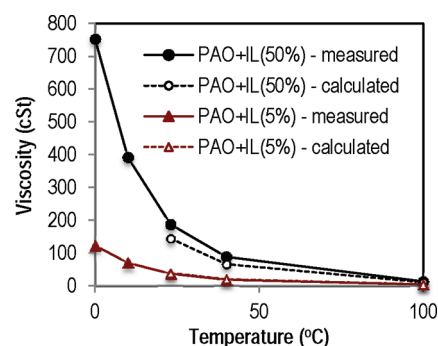


Figure 3. Measured viscosities of oil-IL blends compared with calculated values using Refutas equation.

or small anions, e.g., bis(tetrafluoromethylsulfonyl)imide (Tf_2N), and thus cannot dissolve in oils. Our experiments also found that, in addition to the quaternary structures, an oil-miscible IL needs to contain at least one alkyl with four carbons or more for both the cation and the anion. The phosphate IL reported by Mori's group in¹¹ has a similar structure to $[P_{66614}][DEHP]$ but its alkyls on the anion are so short (one carbon each) that we suspect a limited solubility in oils.

3.4. Antiscuffing and Antiwear Functionality. The lubricating performance of the oil-IL blends was benchmarked against that of the PAO and 5W-30 synthetic oils. The friction curves and wear rates are presented in Figure 4 and Table 3,

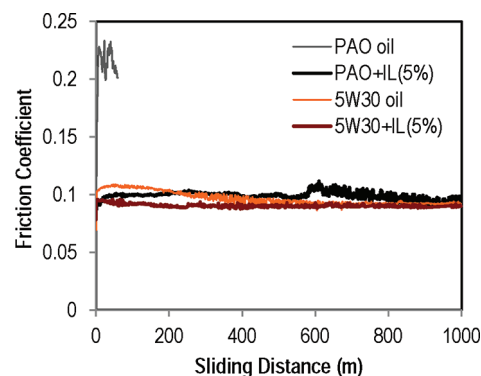


Figure 4. Friction behavior of oils with and without addition of $[P_{66614}][DEHP]$.

Table 3. Comparison of Wear Rates

lubricant	viscosity (cSt, 23 °C)	wear rate ($mm^3/(N m)$)	
		liner	ring
PAO 4 cSt base oil	34.5	$5.9 \pm 4.7 \times 10^{-4}$	$>1.0 \times 10^{-6}$
PAO+IL(5%)	36.6	$5.6 \pm 3.5 \times 10^{-7}$	$1.4 \pm 0.5 \times 10^{-8}$
5W-30 engine oil	140.9	$4.7 \pm 0.3 \times 10^{-7}$	$6.6 \pm 4.9 \times 10^{-9}$
5W-30+IL(5%)	149.9	$1.3 \pm 0.2 \times 10^{-7}$	$2.0 \pm 1.6 \times 10^{-9}$

respectively. Each curve or data point represents the average value from two tests.

The friction coefficient for the PAO oil started around 0.1, but quickly transitioned to above 0.2 and then fluctuated between 0.2 and 0.25. This sharp friction transition is a classic indication of lubrication failure leading to contact surface scuffing and the following high fluctuation at a high friction level

implies the propagation of scuffing damage. The dominating flakelike features on the worn liner surface (Figure 5a) confirmed

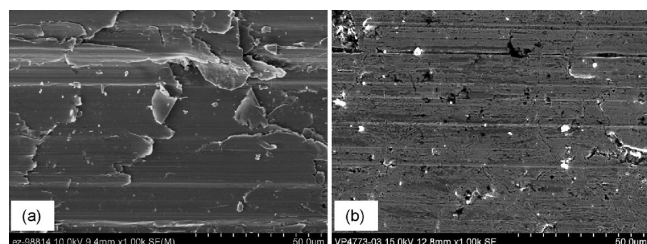


Figure 5. SEM images of the worn cast iron surfaces lubricated by (a) PAO oil and (b) PAO+IL(5%) blend.

the scuffing-associated adhesive wear and plastic deformation. In contrast, the PAO-IL blend produced a relatively stable friction coefficient around 0.1 throughout the entire test (Figure 4) and the wear scar showed mild abrasive wear with no scuffing damage (Figure 5b). As compared in Table 3, the wear rates of the rubbing metallic surfaces were 3 orders of magnitude in difference for the PAO oil with and without the IL additive.

In spite of being only a single additive blend, PAO+IL(5%) performed nearly as well as the fully formulated 5W-30 engine oil in both friction and wear perspectives (Figure 4 and Table 3). It is worth noting that the PAO-IL blend has a much lower viscosity (36.6 cSt) compared to the 5W-30 engine oil (140.9 cSt). This suggests that the IL additive may potentially allow the usage of lower viscosity engine oil, which in turn improves the engine efficiency by reducing churning losses.

[P₆₆₆₁₄][DEHP] was also added into the 5W-30 engine oil to investigate its compatibility with a commercial oil additive package. While little change was observed in friction behavior, the wear rates were decreased by ~70% for both sliding surfaces (Table 3). This implies a possible synergistic effect between the IL and the existing antiwear additives, especially zincdialkyl-dithiophosphate (ZDDP).¹⁸ A typical ZDDP molecule is illustrated in Figure 6.

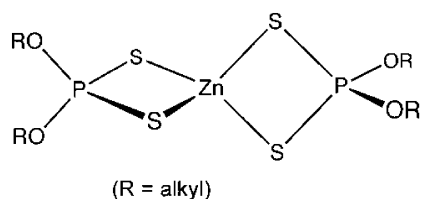


Figure 6. Molecular structure of ZDDP.

The antiwear mechanism of ZDDP is to form a protective boundary film on a metallic bearing surface in a thickness from tens to a couple of hundred nanometers.^{18,19} IL-produced tribo-boundary films were also detected on both ferrous and aluminum surfaces, and their thicknesses, nanostructures, and compositions have recently been reported to be material dependent.²⁰

In this study, screening EDS chemical analysis from the top surface (under SEM) was first conducted and the spectra indicated P content on the wear scar lubricated by PAO+IL, and P, S, and Zn on the wear scar lubricated either by the 5W-30 engine oil or by the 5W-30+IL blend. No phosphorus was detected outside the wear scar. This is in line with the literature observation that tribo-film formation requires thermomechanical

excitations.^{18–20} Cross-sectional TEM examination and EDS chemical analysis were then conducted on the cast iron worn surfaces to provide in-depth characterization of the tribo-boundary films.

The TEM image in Figure 7a shows a cross-section of the near surface region underneath the wear scar lubricated by

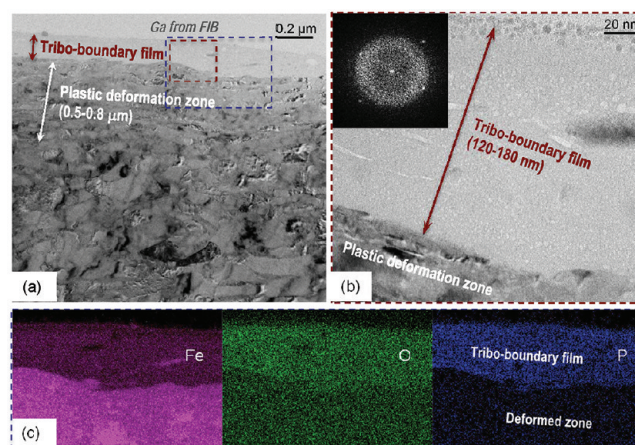


Figure 7. (a, b) TEM imaging and (c) EDS element mapping on the cross-section of the near surface zone of a cast iron worn surface lubricated by PAO+IL(5%). b and c correspond to the red dash line box and blue dot line box marked on a, respectively.

PAO+IL(5%). It clearly shows a two-layer structure including a top tribo-boundary film (120–180 nm) and a subsurface plastic deformation zone (0.5–0.8 μm) with a refined grain structure. This protective boundary film is believed to be responsible for the antiscuffing/antiwear functionality provided by the IL additive. The higher-magnification image of the boundary film in Figure 7b (corresponding to the red dashed box in Figure 7a) reveals an amorphous matrix embedded with fine nanoparticles (1–10 nm in diameter), and the electron diffraction pattern (insert in Figure 7b) confirms the nanocomposite phase structure. The EDS element mapping in Figure 7c (corresponding to the blue dashed box in Figure 7a) shows high concentrations of P, O, and Fe in the boundary film as a result of interactions between the IL and the metal surface.

For comparison, the cross-sectional TEM examination and EDS analysis for the worn surface lubricated by the 5W-30 engine oil are shown in Figure 8. A similar two-layer structure was observed with a tribo-boundary film in the thickness of 40–60 nm and a subsurface deformation zone in the thickness of 0.9–1.2 μm. The boundary film is dominated by an amorphous phase containing nanocrystals, as revealed by the high-magnification TEM image and electron diffraction pattern in Figure 8b. High concentrations of Zn and S in the tribo-boundary film (Figure 8c) suggest a contribution from the oil additive package, specifically ZDDP, to film formation. However, little P (another active element of ZDDP) was detected.

Figure 9 shows the nanostructure and chemical composition of the tribo-boundary film (250–350 nm) and plastic deformation zone (1.8–2.3 μm) when both [P₆₆₆₁₄][DEHP] and ZDDP were present (5W-30 + 5%IL). Again the boundary film is nanocomposite in nature (amorphous matrix containing nanocrystals). According to the EDS element mapping in Figure 9c, this tribo-boundary film is rich in S and Zn as well as P. This suggests involvement of both [P₆₆₆₁₄][DEHP] and

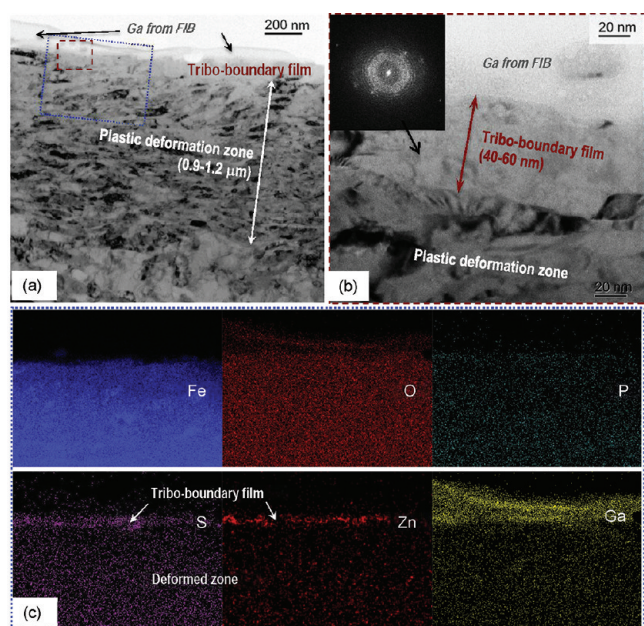


Figure 8. (a, b) TEM imaging and (c) EDS element mapping on the cross section of the near surface zone of a cast iron worn surface lubricated by SAE SW-30 engine oil. b and c correspond to the red dash line box and blue dot line box marked on a, respectively.

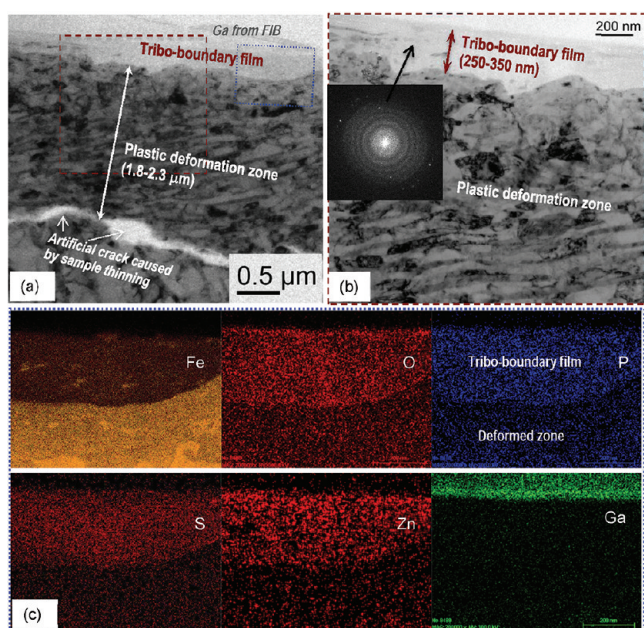


Figure 9. (a, b) TEM imaging and (c) EDS element mapping on the cross-section of the near surface zone of a cast iron worn surface lubricated by SW-30+IL(5%). b and c correspond to the red dash line box and blue dot line box marked on a, respectively.

ZDDP in film formation, which confirms their synergistic effects on wear reduction (Table 3).

Although the three surfaces described above have similar layered structures, the layer thicknesses are quite different:

- Tribo-boundary film: ZDDP < IL < ZDDP+IL
- Plastic deformation zone: IL < ZDDP < ZDDP+IL

Although localized layer thickness measurement may not be representative (sampling is always an issue for TEM

examination), the trend is worth noting. It is known that ZDDP requires high contact pressure and/or elevated temperature to break down into Zn^{2+} and dialkyl-dithiophosphate (DDP^-) before reacting with the metallic surface to form a boundary film.^{18,19} In contrast, the IL additive is naturally in an ionic form, which may allow a more efficient film formation process than ZDDP, leading to a thicker boundary film. The thickness of the film formed in ZDDP+IL is more than the sum of the two formed separately.

The thickness difference in the plastic deformation zones may be explained by energy dissipation. Wear (localized fracture and delamination) and plastic deformation are the two major energy dissipation sources in steady-state sliding dominated by plowing rather than adhesion.²¹ Because nonscuffed lubricated sliding usually involves little adhesion, all frictional energy in the tests could be assumed to dissipate through material removal and plastic deformation. The steady-state friction coefficients of these three lubricants were comparable (Figure 4), meaning there was a similar amount of energy input. Thus, one can expect a lower wear rate coupled with a thicker plastic deformation layer, which has been confirmed by measurements: the wear rate ranking IL > ZDDP > ZDDP+IL (Table 3) is in the opposite order of the deformation zone thickness (Figures 7–9).

CONCLUSION

[P₆₆₆₁₄][DEHP] was synthesized, characterized, and evaluated as a candidate lubricant additive. It is hydrophobic and stable in presence of water as well as in ambient environment. This IL distinguishes itself from most other ILs by its oil-miscibility and noncorrosiveness. It possesses higher thermal stability and comparable wettability on solid surfaces compared to hydrocarbon oils. Laboratory tribological testing demonstrated superior anti-scuffing, antiwear functionality for this IL additive in a synthetic base oil. The best wear performance was achieved when mixing the IL with a fully formulated engine oil, indicating a synergistic effect with existing oil additives. Cross-sectional nanostructural examination and chemical analysis of the near surface region revealed a similar layer structure, including a top tribo-boundary film and a subsurface plastic deformation zone, for the worn surfaces generated in the IL- and/or ZDDP-containing lubricants. Initial characterization and testing results suggest substantial potential for using this oil-miscible IL as an antiwear additive in lubrication.

AUTHOR INFORMATION

Corresponding Author

*Address: P.O. Box 2008, MS-6063, Oak Ridge, TN 37831-6063. Tel: (865) 576-9304. E-mail: qujn@ornl.gov.

Notes

The authors declare no competing financial interest.

ACKNOWLEDGMENTS

The authors thank D.W. Coffey, Dr. H. Xu, and Dr. S.R. Hunter for FIB-aided TEM sample preparation, SEM imaging, and help on contact angle measurement, respectively. Research sponsored by the Vehicle Technologies Program, Office of Energy Efficiency and Renewable Energy, U.S. Department of Energy (DOE). Part of the IL synthesis effort was supported by the DOE Office of Basic Energy Sciences, Division of Chemical Sciences, Geosciences, and Biosciences. The characterization work was supported in part by ORNL's SHaRE User Facility, which is sponsored by the DOE Office of Basic Energy Sciences.

B.Y. and D.G.B. acknowledge the Oak Ridge Associated Universities for postdoctoral fellowships.

■ REFERENCES

- (1) Tung, S. C.; McMillan, M. L. *Tribol. Int.* **2004**, *37*, 517–536.
- (2) Rudnick, L.R. *Lubricant Additives – Chemistry and Applications*; Marcel Dekker: New York, 2003.
- (3) Holbrey, J. D.; Seddon, K. R. *Clean Prod. Process.* **1999**, *1*, 223–236.
- (4) Ye, C.; Liu, W.; Chen, Y.; Yu, L. *Chem. Commun.* **2001**, 2244–2245.
- (5) Qu, J.; Truhan, J.J.; Dai, S.; Luo, H.M.; Blau, P.J. *Lubricants or Lubricant Additives Composed of Ionic Liquids Containing Ammonium Cations*. U.S. Patent 7 754 664.
- (6) Qu, J.; Truhan, J. J.; Dai, S.; Luo, H. M.; Blau, P. J. *Tribol. Lett.* **2006**, *22*, 207–214.
- (7) Jiménez, A. E.; Bermudez, M. D.; Iglesias, P.; Carrion, F. J.; Martinez-Nicolas, G. *Wear* **2006**, *260*, 766–782.
- (8) Jiménez, A. E.; Bermudez, M. D. *Wear* **2008**, *265*, 787–798.
- (9) Qu, J.; Blau, P. J.; Dai, S.; Luo, H. M.; Meyer, H. M. III. *Tribol. Lett.* **2009**, *35*, 181–189.
- (10) Mistry, K.; Fox, M. F.; Priest, M. *J. Eng. Tribol.* **2009**, *223*, 563–569.
- (11) Lu, R. G.; Nanao, H.; Kobayashi, K.; Kubo, T.; Mori, S. *Jpn. Petrol. Inst.* **2010**, *53*, 55–60.
- (12) Schneider, A.; Brenner, J.; Tomastik, C.; Franek, F. *Lubr. Sci.* **2010**, *22*, 215–223.
- (13) Yao, M. H.; Liang, Y. M.; Xia, Y. Q.; Zhou, F. *ACS Appl. Mater. Interfaces* **2009**, *1*, 467–471.
- (14) Cai, M. R.; Liang, Y. M.; Yao, M. H.; Xia, Y. Q.; Zhou, F.; Liu, W. M. *ACS Appl. Mater. Interfaces* **2010**, *2*, 870–876.
- (15) Sun, J. Z.; Howlett, P. C.; MacFarlane, D. R.; Lin, J.; Forsyth, M. *Electrochim. Acta* **2008**, *54*, 254–260.
- (16) Hamrock, B.J.; Dowson, D., *Ball Bearing Lubrication – The Elastohydrodynamics of Elliptical Contacts*; John Wiley & Sons: New York, 1981.
- (17) Maples, R.E. *Petroleum Refinery Process Economics*, 2nd ed.; PennWell Books: Tulsa, OK, 2000.
- (18) Nicholls, M. A.; Do, T.; Norton, P. R.; Kasrai, M.; Bancroft, G. M. *Tribol. Int.* **2005**, *38*, 15–39.
- (19) Qu, J.; Blau, P. J.; Howe, J. Y.; Meyer, H. M. III. *Scr. Mater.* **2009**, *60* (10), 886–889.
- (20) Qu, J.; Chi, M.; Meyer, H. M. III.; Blau, P. J.; Dai, S.; Luo, H. *Tribol. Lett.* **2011**, *43* (2), 205–211.
- (21) Rigney, D. A.; Hirth, J. P. *Wear* **1979**, *53*, 345–370.